Chemical Geology 253 (2008) 130–135

Contents lists available at ScienceDirect

Chemical Geology

journal homepage: www.elsevier.com/locate/chemgeo

Metal and proton binding onto the roots of *Fescue rubra*

Brian R. Ginn *, Jennifer S. Szymanowski, Jeremy B. Fein

Department of Civil Engineering and Geological Science, 156 Fitzpatrick Hall, University of Notre Dame, Notre Dame, IN 46556, USA

ARTICLE INFO

Article history:
Received 15 December 2007
Received in revised form 8 April 2008
Accepted 3 May 2008

Editor: D. Rickard

Keywords:
Grass
Root
Adsorption
Cadmium
Lead
Surface complexation

ABSTRACT

This study quantifies Pb and Cd adsorption onto the root cell walls of the grass species *Festuca rubra* by applying a surface complexation approach to model the observed adsorption behavior. We use potentiometric titrations to determine deprotonation constants and site concentrations for the functional groups on the root material. We model the acid/base properties of the root cell wall with a non-electrostatic model involving three discrete surface functional group types, with pK_a values of 4.2±0.1, 6.2±0.2, and 8.8±0.2. Pb adsorption kinetics experiments indicate that the experimental systems reach equilibrium within 3 h, and Pb desorption experiments indicate that the adsorption reactions are fully reversible on this time scale. Adsorption experiments conducted as a function of pH yield site-specific stability constants for the important Pb- and Cd-root surface complexes. The results of the Pb and Cd adsorption experiments indicate that the first two sites contribute to metal adsorption under the experimental conditions, with calculated log stability constant values of 4.1±0.3 and 5.9±0.3 for the Pb system; and 3.5±0.4 and 5.0±0.5 for the Cd system. Our results suggest that the stabilities of the Pb- and Cd-surface complexes are comparable to those involving other biomass surfaces, and therefore these complexes may affect the transport and distribution of metals in soil systems.

1. Introduction

Understanding the fate and bioavailability of heavy metals in soils depends on our ability to accurately describe the distribution of the metals between a number of possible reservoirs. Heavy metals can exist as metal precipitates, as aqueous species, or as surface complexes on sorbents such as mineral surfaces, bacteria, fungi, solid organic matter, and plant roots. There have been a number of studies of the adsorption of metals onto plant material (e.g., Gardea-Torresdey et al., 1998; Keskinkan et al., 2004; Abia and Igwe, 2005; Fritioff and Greger, 2006; and Araújo et al., 2007). These studies primarily focused on bulk metal adsorption onto the entire plant. However, Fritioff and Greger (2006) determined the proportion of metal uptake that was found on the roots of the pondweed species *Potamogeton natans* relative to the rest of the plant. They found that Zn, Cu, and Pb adsorbed significantly more onto the roots of the plants than the stem and leaves, but Cd adsorbed similarly onto all three parts. Araújo et al. (2007) performed metal adsorption experiments using roots of the grass species *Paspalum notatum*. In each of the previous studies of metal binding by plant material, the adsorption experiments were modeled using either Freudlich or Langmuir isotherm approaches, making it problematic to extrapolate the results to conditions not directly studied in the laboratory.

Spectroscopy and biochemical assay studies suggest that metal cations bind to carboxyl functional groups on the root cell walls of the alfalfa species *Medicago sativa* at pH 7 (Tiemann et al., 1999; Parsons et al., 2002; Gardea-Torresdey et al., 2002), but it is possible that other sites are present and active under other pH and experimental conditions. Furthermore, none of the previous studies of metal adsorption onto plant root material apply a modeling approach that can be incorporated into thermodynamic models of metal speciation and transport in soil systems. Therefore, while previous studies document the potential importance of plant and root material in the passive binding of aqueous metal cations, the results of these studies are applicable only to the experimental conditions of each study, and cannot be generalized in order to predict metal speciation and transport for other systems of environmental interest.

Surface complexation models (SCMs) quantify the thermodynamic stability of the important metal-surface complexes, and hence can be used to estimate metal distributions as a function of a range of physical and chemical conditions (e.g., Hohl and Stumm, 1976). SCMs were initially developed to apply to mineral surfaces, but they have been extended to bacterial surfaces (Hohl and Stumm, 1976; Plette et al., 1995; Fein et al., 1997; Daughney et al., 2001; Haas et al., 2001; Kaulbach et al., 2005) as well as to the algal species *Pseudokirchneriella subcapitata* (Kaulbach et al., 2005) and the fungal species *Saccharomyces cerevisiae* (Naeem et al., 2006). Calculations of the importance of a particular type of sorbent in binding a metal of interest using a surface complexation model require knowledge of the number of functional group types present on the sorbent, the deprotonation constants and site concentrations of each of these functional groups, and the thermodynamic stability constants for the important metal-

* Corresponding author.
E-mail address: bginn@nd.edu (B.R. Ginn).

0009-2541/$ – see front matter © 2008 Elsevier B.V. All rights reserved.
doi:10.1016/j.chemgeo.2008.05.001

surface complexes that involve these functional groups on the surface of interest.

In this study, we extend the SCM approach to model the adsorption behavior of plant root material. We perform potentiometric titrations and Cd and Pb adsorption experiments using the roots of a common grass species, *Festuca rubra* (red fescue grass). Roots are the part of the plant likely to control metal–grass interactions because they absorb water and are in contact with the soil. The rest of the plant will not adsorb metals because it is covered with a hydrophobic cuticle and is not directly in contact with soil or groundwater. Although grass roots as a whole have lower surface area to volume ratios than prokaryotic cells, they may exhibit similar metal binding properties because soil pore water has access to every cell within the root. The root cells are surrounded by a continuous cell wall matrix that allows water to quickly diffuse throughout the interior of the root (but external to each individual cell). The cell wall material and the fluid it contains are called the apoplasm of the root. Thus, any heavy metal present in soil can be bound within the apoplasm of the root, but still be outside the plasma membranes of the individual root cells. On a per gram mass basis, therefore, plant roots may have just as many similar concentrations of cell wall functional groups exposed to soil pore water as smaller organisms despite possessing a smaller surface area.

We determine site concentrations, acidity constants and metal-site stability constants for the important Pb- and Cd-surface complexes, and our results enable comparisons with analogous stability constants for bacterial, algal, and fungal surfaces. These comparisons allow us to gauge the potential importance of different Pb and Cd reservoirs in soils, and the results may also prove useful for modeling and improving efficiency of bioremediation technologies that use grass roots as a metal sorbent material.

2. Methods

2.1. Root preparation

F. rubra, a shade-tolerant, cool season grass, was grown from commercially supplied seed in 25.4 cm deep pots using commercially supplied potting soil. The pots were placed in a natural light, temperature-controlled greenhouse (20 °C), and were watered three times a week. The grass was allowed to grow for approximately 1 month before being harvested. Grass was not cut during growth, and reached an approximate length of 32 cm when harvested. Plugs of grass and soil were removed from the pots and rinsed with tap water to remove as much soil material as possible. Afterwards, individual root fibers were cut from the rest of the plant, and were rinsed repeatedly in 18 MΩ ultrapure water to remove soil debris from each fiber.

After the initial rinsing, the root fibers were soaked in HNO_3 (pH=2.0) for 30 min to remove strongly bound cations still present from the soil. Our preliminary experiments indicated that potentiometric titration and metal adsorption experiments that were conducted using non-acid washed roots exhibited significantly higher experimental scatter and uncertainty compared to experiments performed using acid-washed roots. After the acid-wash step, the roots were again rinsed three times in ultrapure water. Fig. 1 shows a scanning electron microscope (SEM) image of a sample rinsed in ultrapure water and a sample rinsed in HNO_3 for comparison. There is no apparent structural damage to the root material caused by the acid-wash step.

The roots were blotted with lab tissue to remove as much moisture as possible, and then were allowed to dry, open to the atmosphere, for 2 h. The roots were then cut with cleaned scissors to an approximate length of 2 mm. Cutting of the root material was necessary in order to maintain a suspension of the material during experimentation, and to enable the creation of suspensions with reproducible and known concentrations of root material. Previous studies of metal adsorption onto root material have used a similar cutting technique (e.g., Araújo et al., 2007). Further, due to the highly porous and permeable nature of the root material, it is unlikely that the cutting significantly affected

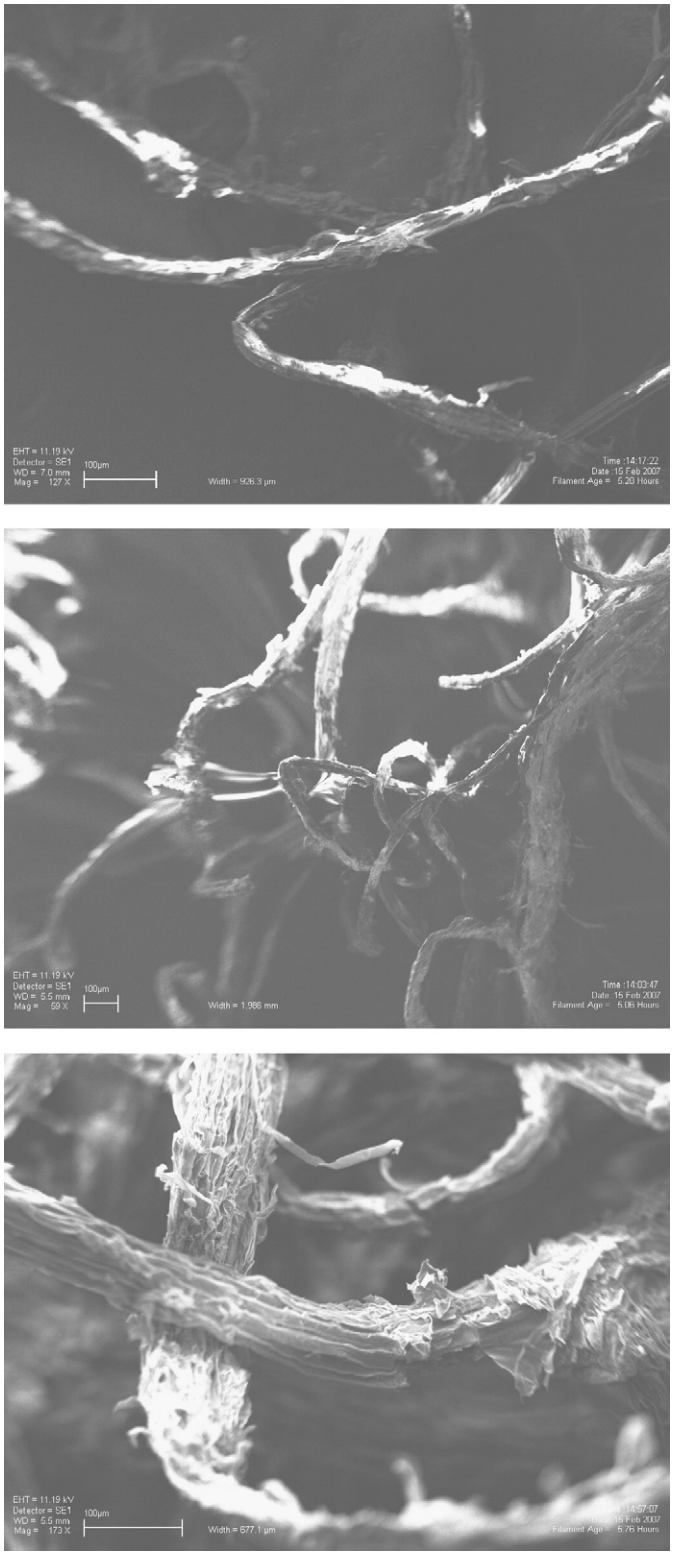

Fig. 1. SEM images of *F. rubra* root material that was washed in water only (top) and *F. rubra* root material that was washed in 0.01 M HNO3 (middle). Neither sample was coated in gold, so any residue organic material from the growth soil shows as bright spots. Note that the water-washed sample exhibits these bright spots, while the acid-washed sample does not. The bottom image is of an acid-washed grass root coated with gold. It shows the structural integrity of the root after our washing procedure.

the surface area of the root cells exposed to the aqueous phase during the experiments. The mass of the root used in each experiment was determined by weighing the experimental solution before and after addition of the air-dried root material.

2.2. Potentiometric titration experiments

The potentiometric titration experiments were conducted using 0.1 M $NaClO_4$ as a background electrolyte in order to buffer ionic strength. The $NaClO_4$ solutions were sparged with nitrogen gas for 30 min prior to use in order to remove dissolved CO_2, and all titrations were performed under a nitrogen atmosphere using an automated titration assembly. Each root–electrolyte suspension was first titrated to a starting pH of approximately 2.2 by adding aliquots of 1.0 M HNO_3. Base titrations were then performed by adding aliquots of 1.0 M NaOH. Titrations were performed to a maximum pH of 9.7 to avoid cellular damage. A glass combination electrode was used for the pH measurements, standardized using four NIST-based buffered standards of pH 2.00, 4.01, 7.00, and 10.01. During each titration, the suspension was allowed to equilibrate after each acid or base addition prior to the addition of the next aliquot of acid or base, with equilibrium operationally defined as a drift of 0.01 mV/s or less, typically requiring 1–2 min. Five forward (from low pH to high pH) titrations were conducted, and back-titrations were performed on two of these suspensions to test for reversibility of the deprotonation reactions.

2.3. Metal adsorption kinetics experiments

Metal adsorption reaction kinetics were measured only for the Pb-bearing systems. The metal solutions were prepared by diluting a 1000 ppm aqueous standard in 0.1 M $NaClO_4$. The root material was suspended in the metal solutions to achieve starting concentrations of 1 g/L of root material and 4.85×10^{-5} M total Pb. The suspension was evenly mixed using a Teflon-coated stir bar. Small aliquots of 0.1 N HNO_3 and 0.1 N NaOH were added to control and maintain a constant pH of 5.5 ± 0.2. Samples of the suspension were removed at measured time intervals, and the sample was filtered through a 0.45 μm pore-size cellulose nitrate membrane.

The filtered aqueous samples were analyzed for remaining Pb content using an inductively coupled plasma optical emission spectroscopy (ICP-OES) technique with standards made using a commercially supplied 1000 ppm Pb standard, diluted using 0.1 M $NaClO_4$ to eliminate matrix effects on the analyses. Analytical uncertainties for the ICP-OES results, determined by repeat analyses of the standards, were approximately ±3%.

2.4. Adsorption/desorption experiments

We conducted separate batch Pb and Cd adsorption experiments using the *F. rubra* root material, measuring metal adsorption as a function of pH at a fixed concentration of root material and ionic strength. The metal solutions were prepared by diluting a 1000 ppm Pb or Cd aqueous standard with 0.1 M $NaClO_4$. The root material was suspended in the metal solutions to achieve a starting concentration of 1 g/L of root material, and either 4.85×10^{-5} M total Pb or 2.01×10^{-5} M total Cd.

The metal–root suspensions were shaken to insure homogenization, and divided into separate polypropylene test tube reaction vessels. The pH of each experimental solution was adjusted by adding small amounts of either 1.0 N HNO_3 or 1.0 N NaOH. Based on the results of the kinetics experiments, each experimental system was allowed to react on a test tube rotator for 3 h to reach equilibrium, and then the final pH of each solution was measured. The final pH values for the experiments ranged from approximately 2.5 to 7.0 for Pb, and 2.3 to 8.8 for Cd, and control experiments showed that neither Pb nor Cd precipitation occurred under these conditions. Samples of the aqueous phase were taken from each reaction vessel, and filtered and analyzed for remaining Pb or Cd content using the ICP-OES approach described above.

Desorption experiments were conducted for the Pb system only. These desorption experiments were conducted using an identical procedure to the adsorption experiments, except the pH of the parent Pb solution was adjusted to 7.5 before adding the root material. The parent suspension was allowed to react for 3 h at pH 7.5, during which time virtually all of the Pb adsorbed onto the root material. After this adsorption step, the parent suspension was divided into separate test tubes, and the pH was adjusted downward to pH values of 2 to 7 using minute aliquots of 1.0 N HNO_3. The experimental systems were allowed to re-equilibrate for 3 h, and were sampled and analyzed following the same procedures employed for the adsorption experiments.

2.5. Surface complexation modeling

We apply a similar surface complexation modeling approach to the one described by Fein et al. (1997, 2005) to account for the adsorption of protons and metal cations to bacterial surfaces. The acidity of the surface functional groups is modeled via deprotonation reactions of the following stoichiometry:

$$R\text{–}S_i\text{–}H^o \leftrightarrow H^+ + R\text{–}S_i^- \tag{1}$$

where R and S_i represent the root cell wall and a functional group type, respectively. The distribution of protonated and deprotonated functional group sites is quantified via mass balance equations, such as:

$$K_a = \frac{\left[R\text{–}S_i^-\right] a_{H^+}}{\left[R\text{–}S_i\text{–}H^0\right]} \tag{2}$$

where K_a represents the acidity constant, a represents the activity of the subscripted aqueous species, and the brackets represent the concentration of surface sites in moles per liter of solution. Activity coefficients for all surface species are assumed to be equal to unity.

Our modeling approach implicitly assumes that the deprotonation of each type of functional group, S_i, can be represented as a single deprotonation of an organic acid type. We ignore potential ionic strength effects on the surface electric field because all of our experiments were conducted at the same ionic strength. Potentiometric titration experiments are essentially studies of proton adsorption and desorption, yet because the solvent contains the same element as is reacting with the surface of interest, it is impossible to apply a traditional mass balance approach. Instead, one must define a zero proton condition for the root cell wall and account for changes in proton concentrations relative to that condition (Westall et al., 1995). We choose the fully protonated cell wall to represent our zero proton condition, and we use FITEQL 2.0 (Westall, 1982) to solve for the initial state of protonation in each titration.

We represent interactions between aqueous metal cations, M^{m+}, and deprotonated root surface sites as follows:

$$M^{m+} + R\text{–}S_i^- \Longleftrightarrow R\text{–}S_i\text{–}M^{m-1} \tag{3}$$

where $R\text{-}S_i\text{-}M^{m-1}$ represents the metal-functional group surface complex on the root material. The mass balance equation for Reaction 3 is:

$$K_{ads} = \frac{\left[R\text{–}S_i\text{–}M^{m-1}\right]}{a_{M^{2+}}\left[R\text{–}S_i^-\right]} \tag{4}$$

where K_{ads} is the thermodynamic equilibrium constant for Reaction 3. We assume that the metal binding reactions onto *F. rubra* root material have a metal to site ratio equal to 1:1 as is the case for bacteria, fungi, and algae (Fein et al., 1997; Kaulbach et al., 2005;

Naeem et al., 2006). Acid/base potentiometric titration data provide constraints on the number of site types, their K_a values, and their site concentrations. Metal adsorption measurements conducted as a function of pH constrain the number of sites involved in metal binding, the pH range of influence, and the stability constants for the important metal-functional group surface complexes. We use the program FITEQL 2.0 (Westall, 1982) for the equilibrium thermodynamic modeling of the adsorption data, using aqueous Pb and Cd hydrolysis equilibrium constants from Martell and Smith (1977).

3. Results

The potentiometric titration experiments indicate that the root material exhibits significant buffering capacity over a wide pH range (Fig. 2). The potentiometric titration data are plotted in terms of the mass-normalized buffering capacity, or $(C_a\ C_a - C_b\ C_b - [H^+] + [OH^-])/m_{root}$, where C_a and C_b represent the total concentration of acid and base added to the system at each titration point, $[H^+]$ and $[OH^-]$ are the concentrations of H^+ and OH^- in solution at each point, calculated from pH measurements and activity coefficient calculations (see below), and m_{root} is the air-dried mass of the root material. Fig. 2A illustrates that the titration experiments are reproducible, as the curves represent titration data from three separate batches of root material. The titration data depicted in Fig. 2B represent two different titration reversals, conducted using two separate batches of root material. Each type of symbol represents an up-pH titration followed by a down-pH titration on the same sample of root material. There is some hysteresis evident in our titrations. The hysteresis probably results from the slow kinetics of adsorption that is caused by the porous three dimensional nature of the root material. While slow kinetics of adsorption affects our titration experiments, the metal adsorption experiments were able to reach equilibrium due to the longer equilibration times associated with those experiments. We only incorporate the acidity constants and site concentrations of the up-pH titrations in our metal adsorption models.

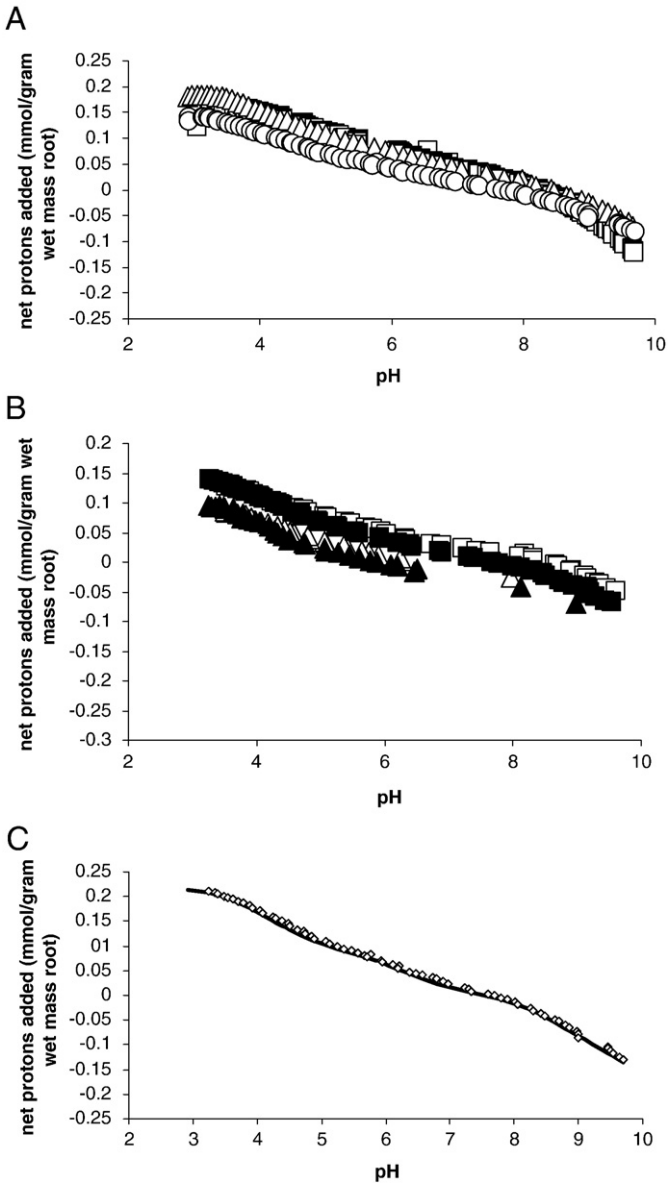

Fig. 2. Potentiometric titration data for experiments with 8.5–20 gm wet mass of root material per liter of 0.1 M $NaClO_4$ electrolyte solution: A) 3 forward (up-pH) potentiometric titrations of *F. rubra* root material; B) Forward (squares) and reverse (triangles) titrations of 2 batches (one batch is represented with unfilled symbols and the other batch is represented with filled symbols) of *F. rubra* root material; C) A typical model fit (solid curve) to one of the five forward titrations of *F. rubra* root material.

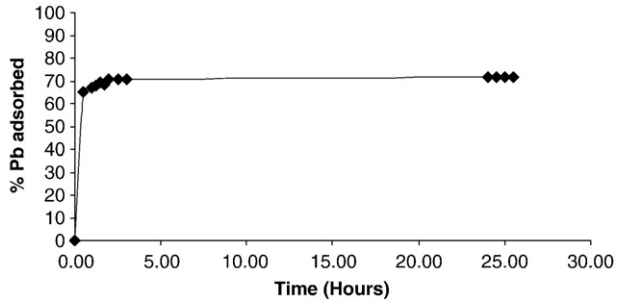

Fig. 3. The measured extent of Pb adsorption onto the root material of *F. rubra* as a function of time. The system contained 10 ppm Pb in a 0.1 M $NaClO_4$ solution, and 1 g/L grass root, and pH was maintained at 5.7 for the duration of the experiment.

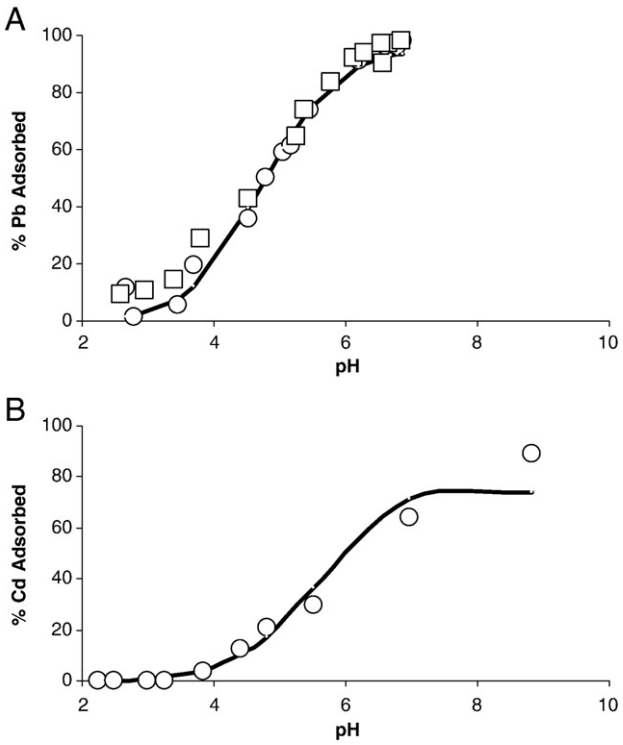

Fig. 4. Adsorption/desorption of Pb (A) and adsorption of Cd (B) onto the root material of *F. rubra*. Circles represent adsorption experiments, and the squares represent desorption results. The solid curves depict the best-fitting models of metal binding to the root material. The experimental systems contained either 10 ppm Pb or 2.3 ppm Cd and 1 g/L grass root material in 0.1 M $NaClO_4$.

Table 1
Results from potentiometric titrations of *F. rubra*

	pK_a 1	pK_a 2	pK_a 3	Site 1 (μmol/g[a])	Site 2 (μmol/g[a])	Site 3 (μmol/g[a])	T_{H0} (μmol/g[a])	$V(Y)$
Titration 1	4.2	6.3	8.9	81	80	161	−270	3.8
Titration 2	4.2	6.3	8.9	81	55	92	−361	5.2
Titration 3	4.3	6.4	8.9	87	58	99	−173	4.8
Titration 4	4.1	6.0	9.0	68	56	83	−460	2.2
Titration 5	4.3	6.2	8.5	86	46	64	−451	2.3
Average	4.2	6.2	8.8	81	59	100		
Standard deviation	±0.1	±0.2	±0.2	±8	±13	±37		

[a] Micrograms per gram wet mass of root material.

Normalized to mass, the *F. rubra* root material exhibits a buffering capacity that is similar to that exhibited by bacterial cells. For example, *Bacillus subtilis* bacterial cells provide a total buffering capacity of approximately 3.0×10^{-4} mol/g over a pH range of 3–10 in 0.1 M $NaClO_4$ (Fein et al., 2005). *F. rubra* has a total buffering capacity of 2.4×10^{-4} mol/g over a similar pH range. The plant roots exhibit a greater buffering capacity than the two other eukaryotic cells that have been titrated in a similar manner. *P. subcapitata* algal cells in 0.1 M $NaClO_4$ provide a total buffering capacity of approximately 4.2×10^{-5} mol/g (Kaulbach et al., 2005), and *S. cerevisiae* fungal cells have a buffering capacity of 1.6×10^{-4} mol/g over this same pH range (Naeem et al., 2006).

Pb adsorption onto the root material is rapid, with most of the adsorption occurring within the first 30 min of the kinetics experiment (Fig. 3). Pb adsorption continues at a slower rate for approximately 2.5 h, at which point a steady-state extent of Pb adsorption is reached and maintained until at least 25.5 h. The observed Pb adsorption equilibration time was longer than is typically observed for bacteria (Fowle and Fein, 2000) and algae (Kaulbach et al., 2005), but is similar to metal adsorption kinetics exhibited by fungi (Naeem et al., 2006). The slow adsorption kinetics may reflect the relative inaccessibility of the porous nature of the root material and the fact that some binding sites are located within this structure.

pH exerts a controlling influence on the extent of both Pb and Cd adsorption onto the root material (Fig. 4), with the extent of adsorption increasing with increasing pH over the pH ranges of approximately 2.5 to 7.0 for Pb, and 2.3 to 8.8 for Cd. The extent of Pb adsorption measured in the desorption experiments shown in Fig. 4A (squares) is within experimental uncertainty of the extent of adsorption measured in the adsorption experiments (circles) for corresponding pH values, indicating that the Pb adsorption reactions are fully reversible on the timescale of these experiments.

4. Discussion

4.1. Titration modeling

We use FITEQL 2.0 (Westall, 1982) modeling to determine the number of discrete functional group site types that are required to account for the observed root material buffering capacity, attempting to fit one-, two-, three-, and four-site models to the potentiometric titration data. The modeling results, a typical fit of which is shown in Fig. 2C for one of the titrations, indicate that for each titration a three-site model yields the best fit to the experimental potentiometric data. Four-site models do not converge for all of the five titration datasets, indicating that the system is under-constrained, and that the data do not support a model with four discrete functional group types. In all cases, a three-site model matches the pH dependence of the buffering capacity significantly better than do models with fewer sites. FITEQL calculates a value for a variance function, $V(Y)$, for each data set, with values closest to 1.0 representing the best fits to the data (Westall, 1982). The calculated $V(Y)$ value improves significantly with each additional site considered in the model to a minimum for the three-site model. Average $V(Y)$ values for the five titrations for the one-, two-, and three-site models are 245, 38, and 6, respectively.

In Table 1, we compile the calculated pK_a values and site concentrations, along with 1 error for each value, for the three-site model for each potentiometric titration and the average values for all the titrations. We also include the value of the initial protonation state, T_{H0}. We use these average values as a foundation for subsequent modeling of the Pb and Cd adsorption data. For the remainder of this paper, because titration data do not yield information on the chemical identity of binding sites, the sites are referred to as they appear in Table 1, as Sites 1–3. The fits to each titration are excellent, with every fit having a $V(Y)$ value of less than 7. A typical model fit is exhibited in Fig. 2C. The pK_a values calculated for each titration are similar, with the largest 1 error equaling 0.2 for Site 3. The variation in site concentrations is comparable to the reported values for bacteria (e.g., Fein et al., 2005).

In Table 2, we compile the average calculated pK_a and site concentrations for *F. rubra*, *B. subtilis*, *P. subcapitata*, and *S. cerevisiae*. Each of these species was titrated using identical procedures, and each set of titration data were modeled using the same discrete site non-electrostatic modeling approach, so the results are directly comparable. Each species contains sites with pK_a values in the ranges 4.4–5.4, 6.4–7.6, and 8.8–9.6. The *F. rubra* root material differs from the other species in that it does not have a site with a pK_a value below 4. The lowest pK_a value in bacteria is often associated with a phosphodiester functional group, which is found in the techoic acid of bacterial cell walls (Guine et al., 2006; Takahashi et al., 2005; Beveridge and Murray, 1980). The cell walls of plants do not possess techoic acids, so the absence of a protonation site with a pK_a value below 4 is not surprising.

4.2. Metal adsorption modeling

The Cd and Pb adsorption behavior onto the root cells was modeled best with the metals forming complexes with Sites 1 and 2. We attempted to account for the observed Cd and Pb adsorption with models that invoke metal binding onto each of the proton-active sites on the root material, singly and in combination, using the FITEQL $V(Y)$ value to constrain the goodness-of-fit of each model. For both the Cd

Table 2
Comparisons between acidity constants and site concentrations for different biomass

Species	Site 1		Site 2		Site 3		Site 4	
	pK_a	μmol/g[d]	pK_a	μmol/g[d]	pK_a	μmol/g[d]	pK_a	μmol/g[d]
F. rubra	N/A	N/A	4.2±0.1	81±8	6.2±0.2	59±13	8.8±0.2	100±37
B. subtilis[a]	3.3±0.2	81±16	4.8±0.1	112±36	6.8±0.3	44±13	9.1±0.2	74±21
S. cerevisae[b]	3.6±0.3	25±12	5.0±0.2	27±15	6.9±0.3	41±14	9.0±0.5	17±18
P. subcapitata[c]	3.9±0.3	6.1±3.0	5.4±0.1	9.8±1.3	7.6±0.3	4.7±1.3	9.6±0.4	7.0±1.4

[a] Gram-positive bacteria; Fein et al. (2005).
[b] Yeast fungal cells; Naeem et al. (2006).
[c] Green algal species; Kaulbach et al. (2005).
[d] Micromoles per gram wet mass of cells.

and the Pb systems, the model that best fits the observed adsorption behavior involves the metal cation of interest binding to deprotonated forms of both Sites 1 and 2. Models with the metal cations binding to only one site type provided significantly worse fits, and models with more than two binding sites for the metal were over-constrained. The model fits to the Cd and Pb data are depicted as solid curves in Fig. 4, and in both cases the two-site models provide reasonable fits to the adsorption data as a function of pH. The model underpredicts Cd adsorption at high pH, suggesting the presence of a Cd-Site 3 complex but the pH range of our data is insufficient to adequately constrain a stability constant for this additional species. The calculated log K values (for a reaction stoichiometry given in Reaction 3) for metal-Site 1 and metal-Site 2 complexes, respectively, are 4.1±0.3 and 5.9±0.3 for the Pb system; and are 3.5±0.4 and 5.0±0.5, respectively, for the Cd system. For the Pb system, both measured adsorption and desorption values were used in these calculations. The uncertainties in K values were determined by finding the range of K values that fit our data set within the certainty of our measurements.

The metal-surface complex stability constant values that we calculate for the root material of *F. rubra* are relatively close to those determined for analogous Cd and Pb complexes involving sites on bacterial, algal, and fungal cell walls. For example, Fein et al. (1997) modeled Pb adsorption onto the bacterial species *B. subtilis* with a Pb-Site 2 log stability constant value of 4.5. Borrok et al. (2004) reported the formation of Cd-Site 2 and Cd-Site 3 complexes on *B. subtilis*, with log stability constants of 3.4 and 4.6, respectively. Kaulbach et al. (2005) reported log stability constant values of 4.1, 5.4, and 6.1 for Cd adsorption onto the first three sites of *P. subcapitata*; and Naeem et al. (2006) determined that Pb and Cd formed surface complexes with Sites 2 and 3 (see Table 2) on the fungal cell wall. They reported log stability constant values of 6.2 and 6.4 for the Pb-Site 2 and Pb-Site 3 complexes, respectively, and values of 4.1 and 4.6 for the corresponding Cd complexes.

Our experiments indicate that the grass species *F. rubra* possesses significant concentrations of proton-active functional groups within the root material, with site concentrations on a per gram basis that are comparable to those found on other forms of soil biomass. The acidity constants for these sites on the *F. rubra* root material are similar to those found for bacteria, algae, and fungi, but the *F. rubra* appears to lack low pH buffering capacity, and hence the lowest pK_a site, that is present on these other forms of biomass. Despite differences in the buffering behavior between *F. rubra* and other forms of biomass, our metal adsorption experiments and modeling results indicate that the grass roots exhibit a roughly similar capacity for metal adsorption as the other forms of biomass. These similarities suggest that a single set of acidity constants and metal binding constants can be used to provide reasonable estimates of metal partitioning onto all forms of soil biomass. If this is true, then it may be possible to consider biomass in general as a single adsorptive reservoir when modeling the distribution of heavy metals in natural soil systems.

Acknowledgement

Research funding was provided by the National Science Foundation through an Environmental Molecular Science Institute grant (EAR02-21966).

References

Abia, A.A., Igwe, J.C., 2005. Sorption kinetics and intraparticulate diffusivities of Cd, Pb and Zn ions on maize cob. Afr. J. Biotechnol. 4, 509–512.
Araújo, G.C.L., Lemos, S.G., Ferreira, A.G., Freitas, H., Nogueira, A.R.A., 2007. Effect of pre-treatment and supporting media on Ni(II), Cu(II), Al(III) and Fe(III) sorption by plant root material. Chemosphere 68, 537–545.
Beveridge, T.J., Murray, R., 1980. Sites of metal deposition in the cell wall of *Bacillus subtilis*. J. Bacteriol. 141, 876–887.
Borrok, D., Fein, J.B., Tischler, M., O'Loughlin, E., Meyer, H., Liss, M., Kemner, K.M., 2004. The effect of acidic solutions and growth conditions on the adsorptive properties of bacterial surfaces. Chem. Geol. 209, 107–119.
Daughney, C.J., Fowle, D.A., Fortin, D., 2001. The effect of growth phase on proton and metal adsorption by *Bacillus subtilis*. Geochim. Cosmochim. Acta 65, 1025–1035.
Fein, J.B., Daughney, C.J., Yee, N., Davis, T., 1997. A chemical equilibrium model for metal adsorption onto bacterial surfaces. Geochim. Cosmochim. Acta 61, 3319–3328.
Fein, J.B., Boily, J.-F., Yee, N., Gorman-Lewis, D., Turner, B.F., 2005. Potentiometric titrations of *Bacillus subtilis* cells to low pH and a comparison of modeling approaches. Geochim. Cosmochim. Acta 69, 1123–1132.
Fowle, D., Fein, J.B., 2000. Experimental measurements of the reversibility of metal–bacteria adsorption reactions. Chem. Geol. 168, 27–36.
Fritioff, Å., Greger, M., 2006. Uptake and distribution of Zn, Cu, Cd, and Pb in an aquatic plant *Potamogeton natans*. Chemosphere 63, 220–227.
Gardea-Torresdey, J.L., Tiemann, K.J., Gonzalez, H.J., Rodriguez, O., Gamez, G., 1998. Phytofiltration of hazardous cadmium, chromium, lead, and zinc ions by biomass of *Medicago sativa* (alfalfa). J. Hazard. Mater. 57, 29–39.
Gardea-Torresdey, J.L., Tiemann, K.J., Parsons, J.G., Gamez, G., Herrera, I., Jose Yacaman, M., 2002. XAS investigation into the mechanism(s) of Au(III) binding and reduction by alfalfa biomass. Microchem. J. 71, 193–204.
Guine, V., Spadini, L., Sarret, G., Muris, M., Delolme, C., Gaudet, J.-P., Martins, J.M.F., 2006. Zinc adsorption to three gram-negative bacteria: combined titration, modeling, and EXAFS study. Environ. Sci. Technol. 40, 1806–1813.
Haas, J.R., Dichristina, T.J., Wade Jr., R., 2001. Thermodynamics of U(VI) sorption onto *Shewanella putrefaciens*. Chem. Geol. 180, 33–54.
Hohl, H., Stumm, W., 1976. Interaction of Pb^{2+} with hydrous α-Al_2O_3. J. Colloid Interface Sci. 55, 281–288.
Kaulbach, E.S., Szymanowski, J.E.S., Fein, J.B., 2005. Surface complexation modeling of proton and Cd adsorption onto an algal cell wall. Environ. Sci. Technol. 39, 4060–4065.
Keskinkan, O., Goksu, M.Z.L., Basibuyuk, M., Forster, C.F., 2004. Heavy metal adsorption properties of a submerged aquatic plant (*Ceratophyllum demersum*). Bioresour. Technol. 92, 197–200.
Martell, A.E., Smith, R.M., 1977. Critical Stability Constants. Plenum, New York, USA.
Naeem, A., Woertz, J.R., Fein, J.B., 2006. Experimental measurement of proton, Cd, Pb, Sr, and Zn adsorption onto the fungal species *Saccharomyces cerevisiae*. Environ. Sci. Technol. 40, 5724–5729.
Parsons, J.G., Gardea-Torresdey, J.L., Tiemann, K.J., Gonzales, J.H., Peralta-Vieta, J., Gonzales, E., Herrera, I., 2002. Absorption and emission spectroscopy investigation of the phyto-extraction of europium(III) nitrate from aqueous solutions by alfalfa biomass. Microchem. J. 71, 175–183.
Plette, A.C.C., van Riemsdijk, W.H., DeWit, J.C.M., Benedetti, M.F., 1995. pH dependent charging behavior of isolated cell walls of a gram-positive soil bacterium. Appl. Geochem. 18, 527–538.
Takahashi, Y., Chatellier, X., Hattori, K.H., Kato, K., Fortin, D., 2005. Adsorption of rare earth elements onto bacterial cell walls and its implications for REE sorption onto natural microbial mats. Chem. Geol. 219, 53–67.
Tiemann, K.J., Gardea-Torresdey, J.L., Gamez, G., Kenneth, D., Renner, M.W., Furenlid, L.R., 1999. Use of X-ray absorption spectroscopy and esterification to investigate the nickel(II) and chromium(III) ligands in alfalfa biomass. Environ. Sci. Technol. 33, 150–154.
Westall, J.C., 1982. FITEQL, a Computer Program for Determination of Chemical Equilibrium Constants from Experimental Data. Version 2.0. Report 82-02. Department of Chemistry. Oregon State University.
Westall, J.C., Jones, J.D., Turner, G.D., Zachara, J.M., 1995. Models for association of metal ions with heterogeneous environmental sorbents 1. Complexation of Co(II) by Leonardite humic acid as a function of pH and $NaClO_4$ concentration. Environ. Sci. Technol. 29, 951–959.